Organic Geochemistry 177 (2023) 104539

Contents lists available at ScienceDirect

Organic Geochemistry

journal homepage: www.elsevier.com/locate/orggeochem

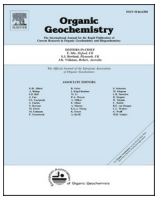

Unusually high production of $C_{37:4}$ alkenone by an Arctic *Gephyrocapsa huxleyi* strain grown under nutrient-replete conditions

Sian Liao [a,b], Karen J. Wang [b,c], Yongsong Huang [c,*]

[a] Department of Chemistry, Brown University, 324 Brook Street, Providence, Rhode Island 02912, USA
[b] Institute at Brown for Environment and Society, Brown University, Providence, Rhode Island 02912, USA
[c] Department of Earth, Environmental and Planetary Sciences, Brown University, 324 Brook Street, Providence, Rhode Island 02912, USA

ARTICLE INFO

Associate Editor–**George Wolff**

Keywords:
Gephyrocapsa huxleyi
$C_{37:4}$%
Isochrysidales
Arctic strain
NIES3366
NIES1312
Sea ice
Culture experiments

ABSTRACT

The percentage of $C_{37:4}$ alkenone relative to total C_{37} alkenones ($C_{37:4}$%) in northern high-latitude ocean waters and surface sediments, which can be up to 77%, has been recently found to correlate strongly with annual mean sea ice coverage. Genomic data and culture experiments suggest these high percentage of $C_{37:4}$ alkenones may be mainly attributed to the production by Group 2i Isochrysidales, because the cosmopolitan Isochrysidales, *Emiliania huxleyi* (recently renamed to *Gephyrocapsa huxleyi*) typically does not produce significant amount of $C_{37:4}$ alkenone in laboratory cultures. However, the presence of significant amounts of C_{38} methyl alkenones in high-latitude ocean sediments and suspended particulate samples suggests possible contributions from *G. huxleyi* as well. Here we performed the first culture experiments on *G. huxleyi* strain NIES3366 from the Chukchi Sea. This strain was isolated from the coldest and highest latitude ocean waters known for *G. huxleyi* strains so far. NIES1312 from the Bering Sea was also cultured under identical conditions for comparison. We show that, in f/2 growth media, NIES3366 was capable of producing unusually large amounts of $C_{37:4}$ alkenone reaching 12.8% at 12 °C and up to 20% between 6 °C and 9 °C. In comparison, NIES1312 only produced 3.6% $C_{37:4}$ at 12 °C. Our results suggest that Arctic strains of *G. huxleyi* may have also contribute to the inventory of the high-$C_{37:4}$ alkenone profile in northern high-latitude oceans. Importantly, however, when NIES3366 was grown in 10 times lower nutrient (f/20) at 12 °C, the $C_{37:4}$% decreased by ~ 50% (to 6%), indicating a strong impact of nutrients on the production of $C_{37:4}$ alkenone. In contrast, salinity levels had a negligible impact on the percentage of $C_{37:4}$ for both strains, indicating an absence of a physiological effect of salinity. We also demonstrate that at low temperatures, tetra-unsaturated alkenones must be included for calculating unsaturation indices to achieve strong linear correlation with temperatures for NIES3366, a feature contrary to other *G. huxleyi* strains isolated from mid- and low- latitude oceans. Our findings provide a refined mechanistic explanation for the application of alkenone $C_{37:4}$% as a quantitative sea ice proxy in high-latitude oceans.

1. Introduction

Alkenones are polyunsaturated long-chain ketones produced by the Isochrysidales, an order of haptophyte algae. For nearly 40 years, unsaturation ratios based on the linear correlation between temperature and degrees of unsaturation of C_{37} methyl (C_{37}Me) alkenones have been widely used for paleo-sea and lake surface temperature (SST) reconstructions (Brassell et al., 1986, 2004; Prahl and Wakeham, 1987; Rosell-Melé and Comes, 1999; Bendle and Rosell-Melé, 2007; Randlett et al., 2014; Longo et al., 2020). Isochrysidales has been classified phylogenetically into three different groups (Theroux et al., 2010; Longo et al., 2016; Wang et al., 2021; Yao et al., 2022), with salinity being the key environmental variable separating their habitats. Group 1 occurs in fresh and oligohaline waters with elevated pH, Group 3 in open ocean with a narrow salinity range, whereas Group 2 has a wide salinity range in saline lakes and marginal oceans (Longo et al., 2016; Yao et al., 2019, 2022). Alkenone distributions produced by the three groups of Isochrysidales differ significantly (Zheng et al., 2019), with one distinct feature that Group 3 species generally do not produce significant amounts of tetra-unsaturated alkenones (Prahl and Wakeham, 1987; Conte et al., 1998; Bendif et al., 2019; Zheng et al., 2019). Here the Group 3 species include *Gephyrocapsa oceanica* and *Emiliania huxleyi*,

* Corresponding author.
E-mail address: yongsong_huang@brown.edu (Y. Huang).

https://doi.org/10.1016/j.orggeochem.2022.104539
Received 15 September 2022; Received in revised form 30 November 2022; Accepted 3 December 2022
Available online 9 December 2022

with the latter being recently renamed to *Gephyrocapsa huxleyi* or *G. huxleyi* (Bendif et al., 2019).

However, sedimentary alkenones in northern high-latitude oceans often display unusually high relative abundance of $C_{37:4}$ and major deviations of $U^{K'}_{37}$-inferred temperatures from annual mean SSTs (Rosell-Melé, 1998; Rosell-Melé and Comes, 1999; Bendle and Rosell-Melé, 2004; Prahl et al., 2010; Rosell-Melé et al. 2011; Méheust et al., 2013; Filippova et al., 2016; Tierney and Tingley, 2018; Max et al., 2020). For example, samples from the northern Japan Sea (Ishiwatari et al., 2001), Okhotsk Sea (Harada et al., 2008), Bering Sea (Harada et al., 2003), Nordic Sea (Bendle and Rosell-Melé, 2004; Bendle et al., 2005) show unusually high abundances of the $C_{37:4}$ alkenone, ranging from 20% to 77% of total C_{37} alkenones. Such high $C_{37:4}$ alkenone abundances are generally absent in waters and sediments from mid- to low- latitude ocean areas or from culture samples of *Gephyrocapsa huxleyi* and *Gephyrocapsa oceanica* (Prahl and Wakeham, 1987; Conte et al., 1998; Müller et al., 1998).

Literature explanations for the unusually high $C_{37:4}$ alkenone profiles observed in high-latitude ocean areas have been vague and sometimes contradictory: e.g., physiological response of *G. huxleyi* to varied salinities/nutrient regimes (Rosell-Melé, 1998; Bendle et al., 2005), existence of other unidentified alkenone producers (Bendle et al., 2005), and oceanic advection of alkenones (Rosell-Melé and Comes, 1999; Filippova et al., 2016). In particular, empirical correlations between sea surface salinity (SSS) and $C_{37:4}$% (lower SSS correlates with higher $C_{37:4}$%) have been observed in the Nordic and Bering Seas in both water column samples and sediments (Rosell-Melé, 1998; Sicre et al., 2002; Sikes and Sicre, 2002; Harada et al., 2003, 2012; Bendle and Rosell-Melé, 2004; Bendle et al., 2005). However, physiological effects of salinity on the production of $C_{37:4}$ have not been supported by culture experiments (Conte et al., 1998; Zheng et al., 2019).

Recently, Wang et al. (2021) recovered abundant DNA sequences of one type of Group 2 Isochrysidales (named 2i, with i referring to ice) in seawater, sea ice and sediment samples from Arctic regions (Wang et al., 2021). They are also found in ice-covered coastal regions such as the Baltic Sea (Enberg et al., 2018; Kaiser et al., 2019) and in saline lakes that experience seasonal or perennial ice cover (Jaraula et al., 2010; Plancq et al., 2019; Wang et al., 2021; Yao et al., 2022). Seasonal time series samples of Group 2i Isochrysidales show a bloom in spring season soon after ice melt in Lake George, North Dakota (Theroux et al., 2020), suggesting Group 2i may be well adapted to grow in low temperature aquatic environments with at least seasonal ice cover. Importantly, a cultured Group 2i strain (Roscoff collection number 5486) was isolated directly from sea ice producing ~ 80% $C_{37:4}$ at 3 °C, with the $C_{37:4}$% insensitive to salinity changes (Wang et al., 2021), as well as temperature changes (Liao and Huang, 2022). Thus, Group 2i Isochrysidales may be primarily responsible for the unusually high $C_{37:4}$ alkenone observed in high-latitude oceans. In fact, Wang et al. (2021) found a strong correlation between $C_{37:4}$% in surface sediments and water column particulate samples and sea ice concentrations, and proposed that $C_{37:4}$% can be used as a quantitative proxy for past sea ice coverage.

The proposed Group 2i production of high amount of the $C_{37:4}$ alkenone in northern high-latitude oceans, however, cannot satisfactorily explain the presence of significant amount of C_{38} methyl ketones (C_{38}Me) in the samples (Wang et al., 2021), as Group 2 Isochrysidales generally produce little C_{38}Me (Zheng et al., 2019). Is it possible that the high abundance of $C_{37:4}$ alkenone in northern high-latitude oceans is produced, at least partially, by *G. huxleyi* which make abundant C_{38}Me (Prahl and Wakeham, 1987; Conte et al., 1998; Zheng et al., 2019)? Are there certain strains of *G. huxleyi*, particularly those isolated from high-latitude oceans, that can produce relatively large amounts of $C_{37:4}$ at low temperatures? So far, the highest $C_{37:4}$% produced by cultured *G. huxleyi* is from strain B92/21 isolated from subarctic Norwegian fjord: ~ 10% at 6 °C (Conte et al., 1998; Zheng et al., 2019). This number is, however, still much lower than many samples found in the Nordic and Bering seas, and hence could not properly explain the unusually high $C_{37:4}$% observed in northern high-latitude oceans.

This research is motivated by the availability of a Chukchi Sea strain of *G. huxleyi*, NIES3366 (Saruwatari et al., 2016). This strain was isolated from the coldest ocean site (shipboard temperature 5.73 °C at the time of sampling) ever for *G. huxleyi* and the only one from the Arctic Ocean at 70.6 °N latitude (Saruwatari et al., 2016). Our objective was to determine the maximum $C_{37:4}$% that can be produced by this strain, especially at low temperatures. Another strain of *G. huxleyi* NIES1312 isolated from Bering Sea at 56.0°N latitude was grown in parallel for comparison, so that we could better examine the strain-to-strain differences in alkenone profiles under identical growth conditions. To better understand how different environmental variables may affect $C_{37:4}$% production, we also grew NIES3366 and NIES1312 at two levels of nutrients (f/2 and f/20) and three different salinities (21, 26, 31 parts per thousand (ppt, or g/kg)). Notably, this is the first time that the effect of salinity on $C_{37:4}$% was experimentally tested for *G. huxleyi*, probably because most of the cultured *G. huxleyi* strains in the past simply did not make significant amounts of $C_{37:4}$ alkenone for such experimental comparison.

2. Materials and methods

2.1. Culture experiments

Gephyrocapsa huxleyi (*G. huxleyi*) strains NIES1312 isolated from Bering Sea (56.0°N, 170.0°W, isolated in October 2002, monthly SST for October was 7.25 °C based on 2001 World Ocean Atlas data, Stephens and Levitus, 2002) and NIES3366 isolated from Chukchi Sea (70.6°N, 168.0°W, isolated during R/V *MIRAI* Arctic Ocean research cruise in October 2010, shipboard temperature during isolation was at 5.73 °C) were purchased from the National Institute for Environmental Studies (Japan) (Saruwatari et al., 2016). At the sampling location for NIES3366, the annual mean SST is 0.58 °C with average June, July, August, September and October SSTs of 0.83, 3.59, 4.73, 3.44, 1.54 °C, respectively (2001 World Ocean Atlas data, Stephens and Levitus, 2002). The region is covered by sea ice from November to June, and has an average ice cover of 79% in 2010 (NOAA/NSIDC Climate Data Record of Passive Microwave Sea Ice Concentration, Version 3, spatial resolution of 25 km × 25 km; Peng et al., 2013). In contrast, at the sampling location for NIES1312, the annual mean SST was 5.16 °C with average June, July, August, September and October SSTs of 5.58, 7.91, 8.96, 8.56, 7.25 °C, respectively (2001 World Ocean Atlas data; Stephens and Levitus, 2002). The region was ice-free in 2002 when this strain was collected (NOAA/NSIDC Climate Data Record of Passive Microwave Sea Ice Concentration, Version 3, spatial resolution of 25 km × 25 km; Peng et al., 2013).

Culture growth conditions and harvest procedures followed those reported in Liao et al. (2020). All species/strains were acclimatized for two weeks before the start of corresponding culture experiments with f/2 (or f/20) medium (Guillard, 1975), which was prepared from seawater collected from Vineyard Sound, Woods Hole, MA, USA at a salinity of 31 ppt (filtered using 0.2 μm Whatman nylon membrane filter and then autoclaved). To study the influence of temperature on alkenone profiles, *G. huxleyi* NIES1312 was cultured at 9, 12, 15, 18, 21 °C at 31 ppt, while *G. huxleyi* NIES3366 was cultured at 0, 3, 6, 9, 12, 15, 18, 21 °C at 31 ppt. For both strains, only one culture experiment was performed at each temperature with no replication because the effect of temperature on alkenone profiles has been shown to be consistent and reproducible over a broad range of temperatures (Conte et al., 1998; Zheng et al., 2016, 2019; Liao et al., 2020). Because the effect of salinity on alkenone profiles in Isochrysidales species is generally very small (e.g., Chivall et al., 2014; Liao and Huang, 2022), culture experiments of *G. huxleyi* NIES3366 and NIES1312 at 21, 26, 31 ppt salinity levels and 12 °C temperature were performed in triplicate.

To study the influence of nutrient concentration on alkenone

profiles, culture experiments of *G. huxleyi* NIES1312 and NIES3366 at 12 °C with f/20 medium were also performed in triplicate. 12 °C was selected as the temperature for salinity and nutrient studies as this is the temperature where both strains show relatively fast growth and NIES3366 shows high $C_{37:4}$% (~ 13%). We did not observe growth for either *G. huxleyi* strain at 12 °C when the salinity was lower than 21 ppt (i.e., 6 and 15 ppt) or higher than 31 ppt (i.e., 35 ppt) and the strain NIES1312 when the temperature was lower than 9 °C at 31 ppt (i.e., 3 °C and 6 °C). The culture experiment for *G. huxleyi* NIES3366 at 0 °C was performed using a self-made ice bath device, as also used in the culture experiments of Group 2i RCC5486 at 0 °C (Liao and Huang, 2022). Cultures were grown under a light:dark cycle set at 16:8h. The light intensity was 17 μmol m^{-2} s^{-1} as both *G. huxleyi* strains prefer low growth light intensities. All cultures experiments were performed in 165 mL of culture medium.

Cultures were harvested at early stationary phase (monitored using hemocytometer counts (Hausser Scientific, PA, USA)) by filtering onto 0.7 μm glass fiber filters (Merck Millipore, MA, USA). All filters were wrapped in aluminum foil and immediately frozen at –20 °C for further extraction and analysis (Zheng et al., 2016; Liao et al., 2020, 2021, 2022).

2.2. Analysis of alkenones

Analysis of culture samples followed the same procedure reported in Liao et al., 2020, 2021. Filters of culture samples were freeze-dried overnight and then sonicated three times with dichloromethane (20 mL DCM, 3 × 30 min) for lipid extractions. Total extracts of culture samples were divided into three fractions using silica gel (230–400 mesh, 40–63 μm) in glass pipettes, and eluted with hexane, DCM and methanol. Alkenones were in the DCM fraction.

DCM fractions were then analyzed on GC-FID (Gas chromatography-flame ionization detection) (Agilent 7890B) and GC–EI-MS (Gas chromatography–electron ionization-mass spectrometry) (Agilent 7890B interfaced to a 5977 Inert Plus MSD) equipped with an RTX-200 column (105 m × 250 μm × 0.25 μm) (Zheng et al., 2017). For the analysis by GC-FID, the carrier gas was hydrogen. Samples were injected under pulsed splitless mode at 320 °C. The initial pulse pressure was 35 psi for the first 1 min. Then the purge flow to split vent was 35.0 mL min^{-1} at 1.1 min. The flow rate (constant flow mode) was 1.5 mL min^{-1}. The initial oven temperature was 50 °C for 2 min, then increased to 255 °C at 20 °C min^{-1}, then increased to 320 °C at 3 °C min^{-1} and held for 35 min. For the analysis by GC–EI-MS, samples were injected under pulsed splitless mode at 320 °C. The initial pulse pressure was 35 psi for the first 0.5 min. The purge flow to split vent was 50 mL min^{-1} at 1.1 min. The flow rate (constant flow mode) was 1.6 mL min^{-1}. The initial oven temperature was 40 °C for 1 min, then increased to 255 °C at 20 °C min^{-1}, then increased to 315 °C at 3 °C min^{-1} and held for 35 min. Samples were analyzed in full-scan mode. The source temperature was 230 °C. The electron ionization energy was 70 eV. The mass range was from *m/z* 50 to 650. Quantification of alkenones was performed using GC-FID. To achieve accurate quantification, concentration of alkenones was adjusted to achieve baseline resolutions of all alkenone peaks (Supplementary Fig. S2-3, S8-9). Analytical error for quantifying alkenone unsaturation ratios using GC-IFD has been reported to be ~ 0.01 (for $U^{K'}_{37}$) or ~ 1% equivalent for individual alkenones (Prahl et al., 1988; Dubois et al., 2009).

2.3. DNA sequencing

To ensure that there were no other Isochrysidales species in the culture experiments, DNA sequencing was performed on filters of culture samples of *G. huxleyi* NIES3366 at 3 °C and 15 °C as well as *G. huxleyi* NIES1312 at 15 °C. Sequencing was performed by Jonah Ventures, Boulder, CO, USA, (https://jonahventures.com/) following procedures reported in Wang et al. (2021).

Only one ESV (deposited in GenBank, accession number OK430883) based on 18S rRNA was identified using the recovered sequences from samples of both *G. huxleyi* NIES1312 and NIES3366, confirming there is no other Isochrysidales species in our culture experiments. 18S rRNA was not sufficient to distinguish between different species in Group 3 due to their low nucleotide substitution rate (Bendif et al., 2014). A representative neighbor-joining tree was constructed using the molecular evolutionary genetics analysis (MEGA) software with 1000 bootstrap replications (Supplementary Fig. S1).

3. Results and discussion

3.1. Growth rates and cell densities at different temperatures, salinities and nutrients

The response of growth rates and cell densities of *G. huxleyi* NIES3366 and NIES1312 to different temperatures shows large differences (Fig. 1a,c; Table 1). While both NIES3366 and NIES1312 achieved the highest cell densities and growth rates at 15 °C to 18 °C, NIES3366 displays much greater tolerance to low growth temperatures (Fig. 1). Specifically, NIES3366 was able to grow at 3 °C or 6 °C, despite low growth rates (the growth rates of NIES3366 at 3 °C or 6 °C were only ~ 40% of the growth rate at 15 °C, Table 1) and long duration (~ 2 months) required to reach stationary phase. NIES1312, in contrast, did not grow at or below 6 °C. NIES3366 also shows extremely slow growth at 0 °C (0.02 d^{-1}). Once below the optimal temperature at 15 °C, growth rates and maximal cell densities of NIES1312 also declined much faster than NIES3366, with maximal cell densities at 9 °C and 12 °C being only 23% of that at 18 °C. The maximal cell density increased from 15 °C to 18 °C by 146% for NIES1312 (3.9×10^6 to 9.6×10^6 cell mL^{-1}) but only by 1% for NIES3366 (7.6×10^6 to 7.7×10^6 cell mL^{-1}), respectively. All these data indicate *G. huxleyi* strain NIES3366 isolated from colder ocean waters is much better adapted to growth in colder conditions. Therefore, the growth characteristics of *G. huxleyi* can differ greatly between different strains, with those isolated from colder settings better adapted to growth in colder temperatures, and vice versa.

Despite NIES3366's ability to grow in relatively low temperatures, we note that the Group 2i strain RCC5486 has far greater preference for growth at exceedingly low temperatures and is a psychrophile (Liao and Huang, 2022). The Group 2i RCC5486 isolated from sea ice displays remarkably fast growth rate at 0–6 °C, which is opposite to NIES3366 whose growth is severely impeded under these low temperatures. The preference for exceedingly low growth temperatures of Group 2i RCC5486 is further exemplified by its inability to grow at 10.5 °C and 12 °C (Liao and Huang, 2022), which is much lower than the optimal growth temperature of 15–18 °C for *G. huxleyi* NIES3366. All these results demonstrate Group 2i strain RCC5486 is, among all three Isochrysidales grown in parallel, the most adapted to growth in cold temperatures. Thus, the association of Group 2i with sea ice and the fact that it blooms during winter and spring is likely dictated by its preference for low temperatures (i.e., it is a psychrophile). We note that the seasonal Isochrysidales successions observed in saline lakes have already shown that Group 2i Isochrysidales peaked in the water column during the early spring soon after melting of lake ice (Theroux et al., 2020).

At 12 °C, growth rates of NIES3366 were at 0.16 d^{-1} for both 26 ppt and 31 ppt, whereas growth rates of NIES1312 were at 0.09 and 0.08 d^{-1}, respectively (Fig. 1b,d; Table 1). However, the growth rate of NIES1312 was ~ 90% higher at 21 ppt than at 31 ppt (Table 1). Higher growth rate at lower salinity has also been observed elsewhere for *G. huxleyi*. For example, growth rate of *G. huxleyi* B92/21 at 24.9 ppt was 109% higher than that at 35.1 ppt at 15 °C (Schouten et al., 2006). At 18 °C, *G. huxleyi* G4 showed ~ 100% faster growth at 20 ppt than at 27 ppt (Fisher and Honjo, 1989). Our preliminary data suggest *G. huxleyi* strains can effectively grow in a broad salinity range between 21 ppt and 31 ppt and

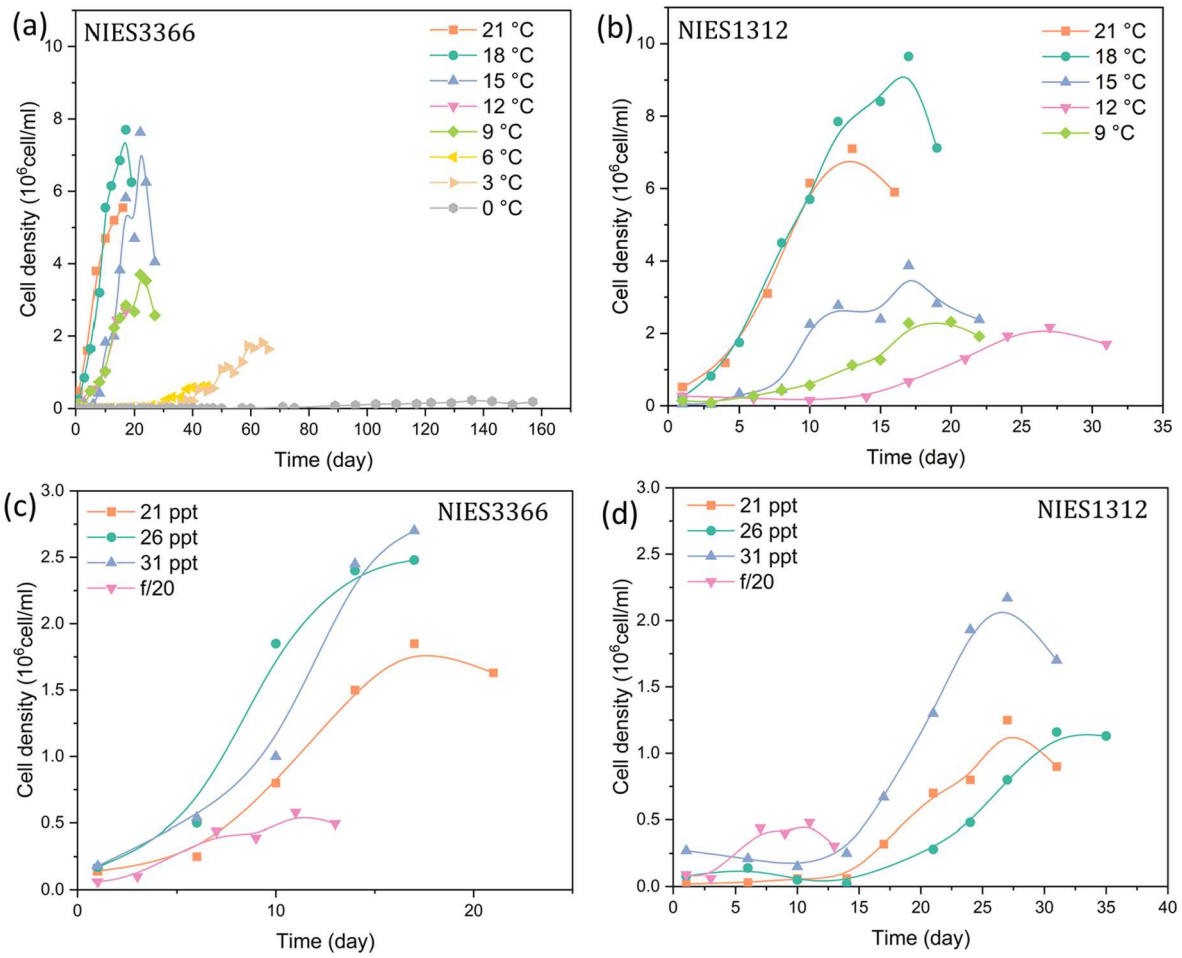

Fig. 1. Growth curves for *G. huxleyi* NIES3366 (a) and NIES1312 (b) at different temperatures. Growth curves for *G. huxleyi* NIES3366 (c) and NIES1312 (d) at different salinities/nutrient concentrations.

growth rate is generally higher at lower salinity levels.

On the other hand, decreasing the nutrient concentrations by 10-fold (using f/20 instead of f/2 culture media) greatly decreased the maximal cell densities for both NIES3366 and NIES1312 strains (Fig. 1; Table 1). Interestingly however, growth rates showed an increase from 0.16 to 0.21 d^{-1} for NIES3366, and 0.08 to 0.15 d^{-1} for NIES1312 when f/2 growth medium is replaced by f/20 medium (or 10 times lower nutrients). Increase of growth rates at lower nutrient concentrations has previously been observed in culture experiments of *G. huxleyi* PML92/11 (Langer and Benner, 2009), suggesting *G. huxleyi* is well adapted to growth in relatively low nutrient waters.

3.2. Effect of temperature on $C_{37:4}$% for G. huxleyi NIES3366 and NIES1312

NIES1312 and NIES3366 exhibit marked differences in their production of tetra-unsaturated alkenones. NIES1312 is akin to common *G. huxleyi* strains isolated from mid-latitude oceans, producing ~ 3–4% $C_{37:4}$ at 9 °C (no growth at 6 °C and lower temperatures; Conte et al., 1998; Zheng et al., 2019). In contrast, NIES3366 displays a remarkable ability to produce large amounts of $C_{37:4}$ alkenone (Fig. 2a). Specifically, NIES3366 produced 11–15% $C_{37:4}$ between 12 °C and 15 °C and 21% to 24% $C_{37:4}$ between 6 °C and 9 °C. We note that the growth rates of NIES3366 slowed dramatically at 0–6 °C (Fig. 1), but our results did show that this alga is physiologically capable of producing even higher amounts of $C_{37:4}$% (34% at 3 °C and 51% at 0 °C) than the $C_{37:4}$% at higher temperature (Fig. 3). In comparison, the highest $C_{37:4}$% among all published *G. huxleyi* culture studies was found for Norwegian fjord strain B92/21 grown at 6 °C using f/2 media, with 10.3% $C_{37:4}$ (Conte et al., 1998).

Despite the high $C_{37:4}$% observed for NIES3366 at low growth temperature in culture, it is questionable whether such alkenone contributions could be realistically produced by Arctic *G. huxleyi* strains in natural settings. NIES3366 was isolated at a time with unusually warm sea surface temperatures of 5.73 °C in October 2010 (Saruwatari et al., 2016). At 6 °C, it took nearly-two months to reach stationary phase with relatively low maximal cell densities in our culture experiments (Fig. 1). Considering that the monthly mean SST of August and September in Chukchi Sea regions are 4.73 °C and 3.44 °C, respectively (2001 World Ocean Atlas data, Stephens and Levitus, 2002), i.e., lower than 5.73 °C, the actual average growth rate and productivity may be quite low (note that culture experiments of NIES3366 were performed in f/2 media with nutrient-replete conditions, in the absence of competition from other algae). In order to test how nutrients might affect the production of $C_{37:4}$ alkenone by NIES3366, we carried out additional growth experiments at lower nutrient conditions.

3.3. Effect of nutrient concentration on $C_{37:4}$% production for G. huxleyi NIES3366 and NIES1312

We found that $C_{37:4}$% decreased dramatically from 13% to 6% for NIES3366 and from 4% to 0.6% for NIES1312 when nutrient concentrations were decreased 10-fold (Fig. 2b,d; Supplementary Fig. S6). Our results indicate that nutrients can strongly affect the production of tetra-unsaturated alkenones in *G. huxleyi* with high concentrations favoring high $C_{37:4}$%. Notably, the concentrations of NO_3^- (88.2 μmol/kg), SiO_2

Table 1
Average daily growth rates and final cell density for NIES3366 and NIES1312 cultured at different temperatures/salinities/nutrient concentrations.

Temperature (°C)	Medium	Salinity (ppt)	Average growth rates (d^{-1})[a]	Initial cell density (10^4 cell/mL)	Highest cell density (10^6 cell/mL)
NIES3366					
21	f/2	31	0.15	48	5.5
18	f/2	31	0.20	25	7.7
15	f/2	31	0.22	6.2	7.6
12	f/2	31	0.16	18	2.7
12	f/2	26	0.16	17	2.5
12	f/2	21	0.15	14	1.8
12	f/20	31	0.21	6	0.6
9	f/2	31	0.16	12	3.7
6	f/2	31	0.07	2.2	0.6
3	f/2	31	0.09	0.6	1.8
0	f/2	31	0.02	2.3	0.2
NIES1312					
21	f/2	31	0.20	52	7.1
18	f/2	31	0.22	24	9.6
15	f/2	31	0.25	5.4	3.9
12	f/2	31	0.08	27	2.2
12	f/2	26	0.09	8	1.2
12	f/2	21	0.15	2	1.2
12	f/20	31	0.15	9	0.5
9	f/2	31	0.14	14	2.3

[a]: $\mu = (\ln(N) - \ln(N_0))/t$, where N is the highest cell density, N_0 is the initial cell density, t is the duration of culture experiment (Schouten et al., 2006).

(10.6 μmol/kg) and PO_4^{3-} (3.6 μmol/kg) in our f/20 medium were still higher (up to 58 times for NO_3^-) than corresponding ocean concentrations (e.g., average concentrations for NO_3^-, SiO_2 and PO_4^{3-} in particulate organic matter (POM) samples of Bering Sea were at 1.5, 9.2 and 0.40 μmol/kg) (Harada et al., 2003). Our data suggest NIES3366 may produce much lower $C_{37:4}$% alkenones in natural Arctic Ocean environments.

Our results from nutrient experiments show opposite trends to those observed in the Bering Sea (Harada et al., 2003). In POM samples from the Bering Sea where up to 41% $C_{37:4}$ has been reported, lower NO_3^-, SiO_2 and PO_4^{3-} nutrient levels are correlated with higher (rather than lower) $C_{37:4}$%, although there is no significant correlation between NH_4^+ concentration and $C_{37:4}$%. (Supplementary Fig. S7). Nutrient limitation experiments have previously been performed on Group 2 Isochrysidales including *I. nuda*, *I. litoralis* and *I. galbana* (Versteegh et al., 2001; Liao et al., 2020). In all cases, $C_{37:4}$% increased for Group 2 species (*I. nuda*, *I. litoralis* and *I. galbana*) at lower nutrient concentrations (Versteegh et al., 2001; Liao et al., 2020), consistent with the trend in POM samples from the Bering Sea (Harada et al., 2003).

In separate experiments, we have shown that Group 2i Isochrysidales is capable of producing ~ 79% of $C_{37:4}$ and can readily thrive at

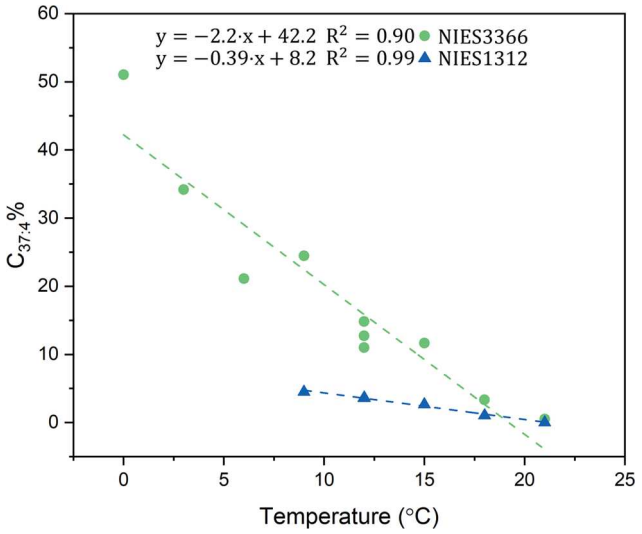

Fig. 3. Influence of temperature on $C_{37:4}$% for *G. huxleyi* NIES3366 and *G. huxleyi* NIES1312. GC chromatograms of the corresponding alkenone profiles are shown in Supplementary Figs. S2, S3.

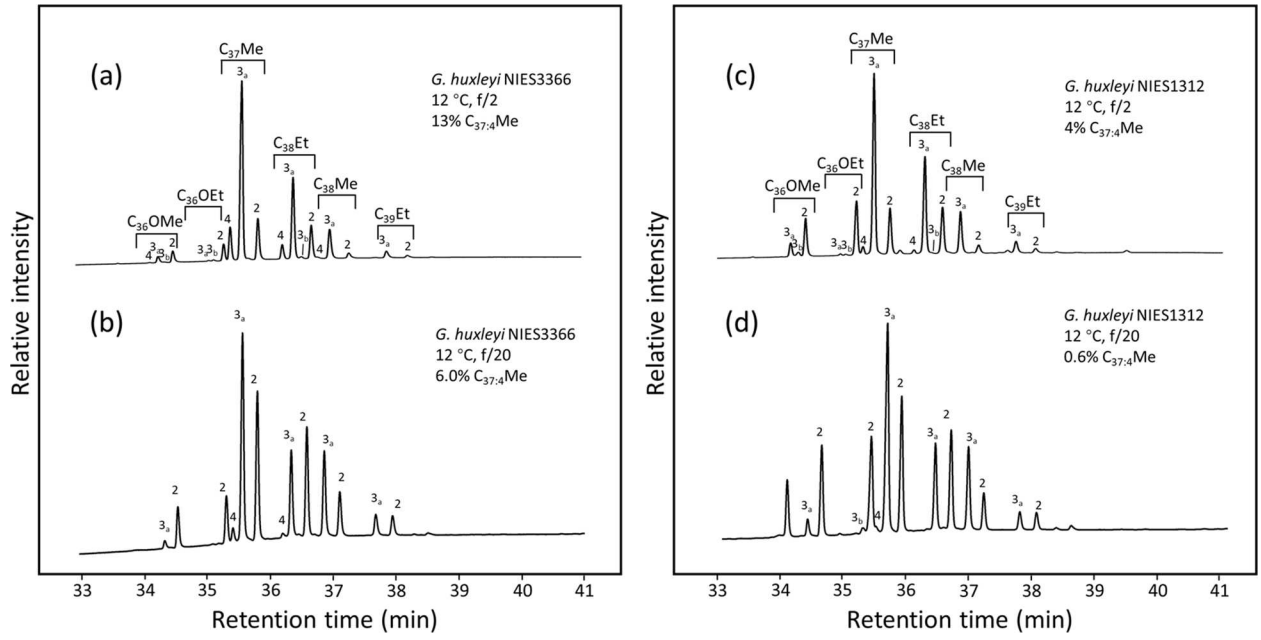

Fig. 2. Gas chromatograms showing the distribution of alkenones and alkenoates for *G. huxleyi* NIES3366 with f/2 medium (a), f/20 medium (b), and *G. huxleyi* NIES1312 with f/2 medium (c) and f/20 medium (d) at 12 °C. Numbers above each peak represent the number of C=C double bonds in corresponding alkenones or alkenoates.

exceedingly low growth temperatures of 0–6 °C (Liao and Huang, 2022). Combined with the exceedingly high $C_{37:4}$% (up to 77%) observed in natural ocean samples (Bendle et al., 2005), it is possible Group 2i Isochrysidales are the main producers of high $C_{37:4}$ alkenones in the northern high-latitude oceans. However, when conditions are suitable, e.g., at unusually warm SSTs and favorable nutrient levels, Arctic strains of *G. huxleyi* like NIES3366 can also occasionally bloom and produce significant amount of alkenones. The sedimentary alkenones could thus be constituted by a combined production by Group 2i Isochrysidales and Arctic strains of *G. huxleyi* in variable percentages, which would explain the wide range of $C_{37:4}$% observed in high-latitude ocean samples, as well as the presence of significant amount of C_{38} methyl ketones.

We note DNA sequences of Group 2i species were not found in seawater samples from the Chukchi Sea and Bering Sea, despite up to 41% of $C_{37:4}$ being reported (Harada et al., 2003; Endo et al., 2018; Wang et al., 2021). The absence of Group 2i DNA is likely due to bias in sampling dates, as seawater samples in the Bering Sea and Chukchi Sea used for DNA sequencing were collected during summer months (Endo et al., 2018; Wang et al., 2021). Group 2i Isochrysidales, however, are likely to bloom in the cold season around the time of sea ice melt (Wang et al., 2021), or soon after lake ice melt in saline lakes (Theroux et al., 2010). Collection of DNA samples in summer may have thus missed Group 2i species.

3.4. Influence of salinity on $C_{37:4}$% for G. huxleyi NIES3366 and NIES1312

In POM samples from the Bering and Nordic seas, a significant increase of $C_{37:4}$% was observed with a slight decrease in salinity (e.g., for Bering Sea, $C_{37:4}$% increased by over 20% when salinity decreased from 32 ppt to 30 ppt) (Harada et al., 2003, 2012; Bendle et al., 2005). Salinity thus remains as one potential factor that may physiologically influence the production of $C_{37:4}$ alkenone profiles by *G. huxleyi* strains.

Our culture experiments at different salinities are the first time that the effect of salinity on the production of $C_{37:4}$ has been examined for *G. huxleyi* species. In both cases, the effects were quite small, compared to the observed changes in ocean samples (Fig. 4; Supplementary Figs. S8 and S9). From 31 to 21 ppt, average $C_{37:4}$% increased slightly for *G. huxleyi* NIES1312 from 3.64 ± 0.04% to 5.49 ± 0.72% (Fig. 4). On the other hand, salinity change from 31 to 21 ppt slightly decreased $C_{37:4}$% from 12.85 ± 1.56% to 10.08 ± 1.46% for *G. huxleyi* NIES3366 (Harada et al., 2003, 2012; Bendle et al., 2005). A number of previous studies

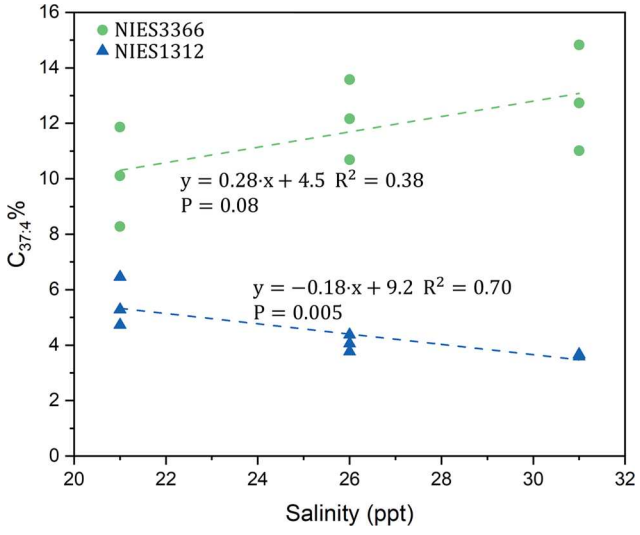

Fig. 4. Influence of salinity on $C_{37:4}$% for *G. huxleyi* NIES3366 and *G. huxleyi* NIES1312 from 21 ppt to 31 ppt at 12 °C. GC chromatograms of the corresponding alkenone profiles are shown in Supplementary Figs. S8, S9.

have shown $C_{37:4}$% produced by Group 2 Isochrysidales also decreases slightly or changes little with decreasing salinity levels (Chivall et al., 2014; Wang et al., 2021). On the other hand, suspended particulate matter (SPM) samples collected from the Nordic Sea (Bendle et al., 2005) and Bering Sea (Harada et al., 2003) showed that $C_{37:4}$% increased by 13.4% and 11.7% per salinity unit decrease, respectively. The amplitude of change observed in the SPM samples far exceeds those observed in our culture experiments (< 3% $C_{37:4}$% change across a 10 ppt salinity gradient; Fig. 4). For NIES3366, the direction of change (i.e., lower salinity corresponds to lower $C_{37:4}$%) is also opposite to the field observations. Therefore, our experimental data do not support the idea of a physiological effect of salinity on $C_{37:4}$ production by both *G. huxleyi* and Group 2 species.

3.5. Correlations between alkenone unsaturation proxies and temperatures for G. huxleyi NIES3366 and NIES1312

In contrast with other *G. huxleyi* strains for which $U^{K'}_{37}$, the most widely used alkenone temperature proxy that is derived from the relative percentage of tri- and di- unsaturated C_{37} methyl ketones, i.e., $U^{K'}_{37} = C_{37:2}/(C_{37:2} + C_{37:3})$, provides better linear correlations than U^{K}_{37} in laboratory cultures (Prahl and Wakeham, 1987; Zheng et al., 2016, 2019): both *G. huxleyi* NIES3366 and NIES1312 yield higher R^2 values of U^{K}_{37} than $U^{K'}_{37}$ (Fig. 5a,b, e.g., for NIES3366, $R^2 = 0.94$ for U^{K}_{37}, 0.82 for $U^{K'}_{37}$). This is consistent with the observations of POM samples from the Nordic Sea (Bendle and Rosell-Melé, 2004; Bendle et al., 2005), and those from laboratory cultures of Group 2 species (Zheng et al., 2016). Notably, for *G. huxleyi* NIES3366, $U^{K'}_{37}$ changed little from 0 °C to 6 °C (0.09 to 0.11), showing a much lower slope than the global core top calibration (Müller et al., 1998). Such small changes in $U^{K'}_{37}$ have also been previously observed for *G. huxleyi* G1779 isolated from the Iceland Basin between 6 °C and 9 °C (0.09 to 0.12) (Conte et al., 1998; Zheng et al., 2019). We note that $U^{K'}_{37}$ values for Group 2i Isochrysidales RCC5486 below 9 °C fall in a similar range and also display little change as temperature decreases (Liao and Huang, 2022; Supplementary Fig. S10). In the global core top calibration, $U^{K'}_{37}$ values are also insensitive to temperature changes below ~ 8 °C (Conte et al., 2006). Such behavior of $U^{K'}_{37}$ values at low temperatures may partially explain the abnormally high $U^{K'}_{37}$-reconstructed SSTs in high-latitude oceans (Bendle and Rosell-Melé, 2004; Bendle et al., 2005; Tierney and Tingley, 2018). Our data suggests U^{K}_{37} is likely a better proxy than $U^{K'}_{37}$ for temperature reconstructions in high-latitude ocean regions.

$U^{K''}_{37}$ has recently been found to provide better linear correlations than U^{K}_{37} and $U^{K'}_{37}$ for Group 2 species (Zheng et al., 2016). Because NIES3366 showed unusually high production of $C_{37:4}$ and higher R^2 of U^{K}_{37} than $U^{K'}_{37}$, similar to Group 2 species (e.g., *I. nuda/litoralis/galbana*) (Zheng et al., 2019; Liao et al., 2020), we also examined the temperature calibrations of $U^{K''}_{37}$ for *G. huxleyi* strains cultured in this work (Fig. 5c). For NIES3366, $U^{K''}_{37}$ ($R^2 = 0.91$) provides comparable R^2 value as U^{K}_{37} ($R^2 = 0.94$), which are both higher than the R^2 values of $U^{K'}_{37}$ ($R^2 = 0.82$). Interestingly, while *G. huxleyi* NIES1312 only produces trace amount of $C_{37:4}$ alkenone, $U^{K''}_{37}$ provides the best linear correlations (highest $R^2 = 0.97$) among three C_{37} proxies examined. Collectively, our data suggest both U^{K}_{37} and $U^{K''}_{37}$ may provide better temperature reconstructions than $U^{K'}_{37}$ in high-latitude oceans.

However, the application of C_{37}-based proxies for temperature reconstructions in high-latitude oceans may be limited to regions without seasonal ice cover (or relatively warm regions). This is because Group 2i species flourish in cool environments which can also contribute to the overall C_{37} alkenone productions, thus biasing the proxy values. Notably, alkenone profiles for Group 2i RCC5486 change little in 0, 3, 6 and 9 °C culture experiments, with average U^{K}_{37}, $U^{K'}_{37}$ and $U^{K''}_{37}$ values at

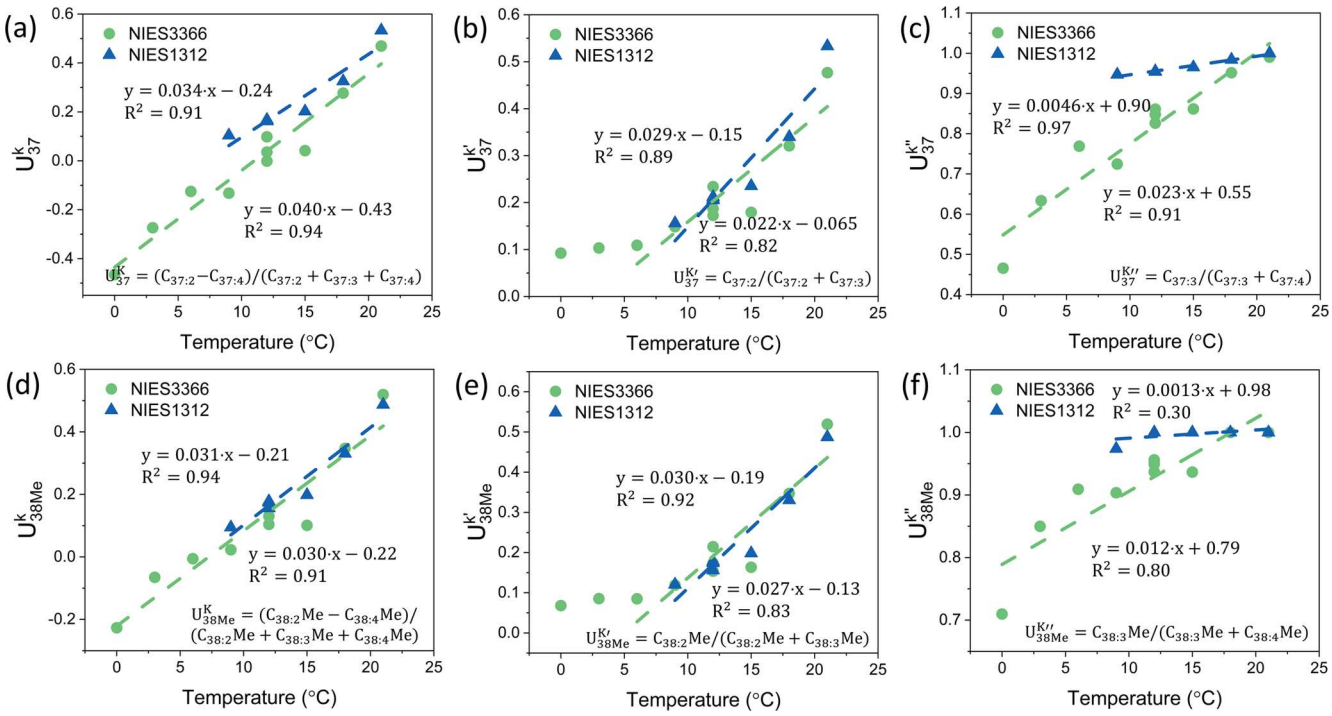

Fig. 5. Temperature calibrations of U^{K}_{37} (a), $U^{K'}_{37}$ (b), $U^{K''}_{37}$ (c), U^{K}_{38Me} (d), $U^{K'}_{38Me}$ (e) and $U^{K''}_{38Me}$ (f) for *G. huxleyi* NIES3366 and *G. huxleyi* NIES1312. Due to little changes in $U^{K'}_{37}$ and $U^{K'}_{38Me}$ values for *G. huxleyi* NIES3366 below 6 °C, linear regressions were performed using data from 6 °C to 21 °C only.

–0.77 ± 0.05, 0.098 ± 0.01 and 0.19 ± 0.04, respectively (Liao and Huang, 2022). These index values are much lower than the corresponding values of NIES3366/NIES1312 in all samples studied in this work, except for $U^{K'}_{37}$ (Group 2i and NIES3366 have similar $U^{K'}_{37}$ values; Supplementary Fig. S10). Temperature reconstructions using C_{37} proxies including $C_{37:4}$ alkenone (i.e., U^{K}_{37} and $U^{K''}_{37}$) may thus result in a record biased towards lower temperatures in the presence of Group 2i species, if a calibration based on *G. huxleyi* as the primary alkenone producer is used. With mixed alkenone production from Group 2i and Group 3 species, proxies based on C_{38}Me alkenones are of particular significance, as Group 2 generally do not produce (or only produce trace amounts of) C_{38}Me alkenones (Zheng et al., 2019; Novak et al., 2022).

Similar to all C_{37}-based proxies, proxy values of $U^{K'}_{38Me}$ of NIES3366 change little for temperatures equal to or < 6 °C (Fig. 5e). U^{K}_{38Me}, on the other hand, shows the highest R^2 values among C_{38}Me proxies examined for both NIES3366 and NIES1312 (Fig. 5d–f, e.g., for NIES3366, R^2 = 0.91 for U^{K}_{38Me}, 0.83 for $U^{K'}_{38Me}$ and 0.80 for $U^{K''}_{38Me}$). U^{K}_{38Me} may thus be more suited than $U^{K'}_{38Me}$ for paleotemperature reconstructions. It is also important to note that among three unsaturation indices based on C_{38}Me alkenones (U^{K}_{38Me}, $U^{K'}_{38Me}$ and $U^{K''}_{38Me}$), changes in salinity and nutrient levels have the smallest impact on $U^{K''}_{38Me}$ values (Supplementary Fig. S1, S12). Therefore, in environmental settings with large variations in nutrient and salinity levels, $U^{K''}_{38Me}$ may also have important advantages over U^{K}_{38Me} and $U^{K'}_{38Me}$.

4. Conclusions

We demonstrate, for the first time, that an Arctic Ocean strain of *Gephyrocapsa huxleyi*, NIES3366, is capable of producing substantially higher amounts of tetra-unsaturated alkenones in nutrient-replete cultures (12% $C_{37:4}$ at 15 °C, 34% $C_{37:4}$ at 3 °C) than all previously cultured *G. huxleyi* strains. In contrast, the *G. huxleyi* strain NIES1312 isolated from the Bering Sea, produces much lower amounts of $C_{37:4}$ (3.1% $C_{37:4}$ on average). Our results suggest that *G. huxleyi* strains isolated from colder ocean sites are intrinsically more likely to produce larger amounts of $C_{37:4}$ alkenone (and other tetra-unsaturated alkenones) than strains isolated from warmer oceans. Both NIES3366 and NIES1312 show highest growth rates and cell densities at 18 °C, much higher than the in situ sea surface temperatures where these strains were isolated (5.73 °C for NIES3366, 7.25 °C for NIES1312). However, the Arctic strain NIES3366 still has much higher tolerance for low growth temperatures than Bering Sea strain NIES1312, with the latter failing to grow at 6 °C, whereas the former is capable of growth between 3 °C and 21 °C. Nevertheless, the growth rates and stationary phase cell densities of NIES3366 are quite low at 6 °C, and especially 3 °C and required ~ 2 months to reach stationary phase in both cases.

In addition, we found nutrient levels in our culture experiments had a strong influence on the production of $C_{37:4}$ for both NIES3366 and NIES1312 strains. Reducing nutrient level by 10-fold (f/2 to f/20 medium) decreased $C_{37:4}$ production from 13% to 6% for NIES3366, and from 4% to 0.6% for NIES1312 at 12 °C. In natural settings with competition from other algae and much lower nutrient levels, it is possible that $C_{37:4}$% produced by NIES3366 would decrease further. The effect of salinity on $C_{37:4}$%, on the other hand, is minimal. Overall, our data suggest that; (1) the productivity of NIES3366 at low temperatures (≤ 6 °C) is likely low and may not be primarily responsible for the observed high $C_{37:4}$ in high-latitude oceans, and (2) the observed increase in $C_{37:4}$% as salinity decreases in Nordic and Bering Sea samples cannot be attributed to the physiological effects of salinity on the production of alkenones by Isochrysidales.

The observed $C_{37:4}$% in natural samples from Nordic and Bering seas ranges from 0% to 77%, with the maximal value greatly exceeding the maximal $C_{37:4}$ production by NIES3366 even at low temperatures (e.g., < 6 °C) and nutrient-replete conditions. Considering that Group 2i Isochrysidales thrive in low temperatures (0–6 °C), and produce high $C_{37:4}$% (70–80%), regardless of growth temperatures and salinities (Liao and Huang, 2022), the high (and highly variable) range of $C_{37:4}$% observed in POM and surface sediment samples in the Bering Sea and Nordic Sea is best explained by a predominant production by Group 2i Isochrysidales, supplemented by certain Arctic strains of *G. huxleyi*. Such combined production also readily explains the high $C_{37:4}$% as well as the

presence of variable amounts of C_{38} methyl ketones in northern high-latitude ocean POM and sediment samples.

Unsaturation indices that exclude tetra-unsaturated alkenones (e.g., $U^{K'}_{37}$, $U^{K'}_{38Me}$) display considerable curvature (flattening) at low growth temperatures for the two *G. huxleyi* strains NIES3366 and NIES1312 in our laboratory cultures. The best linear regressions between unsaturation indices and growth temperatures are obtained for U^{K} and $U^{K''}$ indices that take into consideration of tetra-unsaturated alkenones. Because Group 2i Isochrysidales produce little C_{38} methyl ketones (Zheng et al., 2019), U^{K}_{38Me}, rather than $U^{K'}_{38Me}$, may provide an excellent paleothermometer capable of disentangling the mixed alkenone inputs in high-latitude ocean sediments.

Declaration of Competing Interest

The authors declare that they have no known competing financial interests or personal relationships that could have appeared to influence the work reported in this paper.

Data availability

All data have been provided in the paper

Acknowledgments

This work was supported by the United States National Science Foundation awards to Y.H. (EAR-1762431). We are also grateful for the comments from Associate Editor Prof. George Wolff and three anonymous reviewers, which helped us improve the manuscript.

Appendix A. Supplementary data

Supplementary data to this article can be found online at https://doi.org/10.1016/j.orggeochem.2022.104539.

References

Bendif, E.M., Probert, I., Carmichael, M., Romac, S., Hagino, K., de Vargas, C., 2014. Genetic delineation between and within the widespread coccolithophore morpho-species *Emiliania huxleyi* and *Gephyrocapsa oceanica* (Haptophyta). Journal of Phycology 50, 140–148.

Bendif, E.M., Nevado, B., Wong, E.L.Y., Hagino, K., Probert, I., Young, J.R., Rickaby, R.E. M., Filatov, D.A., 2019. Repeated species radiations in the recent evolution of the key marine phytoplankton lineage *Gephyrocapsa*. Nature Communications 10, 4234.

Bendle, J., Rosell-Melé, A., 2004. Distributions of U^{K}_{37} and $U^{K'}_{37}$ in the surface waters and sediments of the Nordic Seas: Implications for paleoceanography. Geochemistry, Geophysics, Geosystems 5, 19.

Bendle, J., Rosell-Melé, A., 2007. High-resolution alkenone sea surface temperature variability on the North Icelandic Shelf: implications for Nordic Seas palaeoclimatic development during the Holocene. The Holocene 17, 9–24.

Bendle, J., Rosell-Melé, A., Ziveri, P., 2005. Variability of unusual distributions of alkenones in the surface waters of the Nordic seas. Paleoceanography 20, 15.

Brassell, S.C., Eglinton, G., Marlowe, I.T., Pflaumann, U., Sarnthein, M., 1986. Molecular stratigraphy–a new tool for climatic assessment. Nature 320, 129–133.

Brassell, S.C., Dumitrescu, M., Party, ODP Leg 198 Shipboard Party, 2004. Recognition of alkenones in a lower Aptian porcellanite from the west-central Pacific. Organic Geochemistry 35, 181-188.

Chivall, D., M'Boule, D., Sinke-Schoen, D., Sinninghe Damsté, J.S., Schouten, S., van der Meer, M.T.J., 2014. Impact of salinity and growth phase on alkenone distributions in coastal haptophytes. Organic Geochemistry 67, 31–34.

Conte, M.H., Thompson, A., Lesley, D., Harris, R.P., 1998. Genetic and physiological influences on the alkenone/alkenoate versus growth temperature relationship in *Emiliania huxleyi* and *Gephyrocapsa oceanica*. Geochimica et Cosmochimica Acta 62, 51–68.

Conte, M.H., Sicre, M.A., Ruhlemann, C., Weber, J.C., Schulte, S., Schulz-Bull, D., Blanz, T., 2006. Global temperature calibration of the alkenone unsaturation index ($U^{K'}_{37}$) in surface waters and comparison with surface sediments. Geochemistry, Geophysics, Geosystems 7, 22.

Dubois, N., Kienast, M., Normandeau, C., Herbert, T.D., 2009. Eastern equatorial Pacific cold tongue during the Last Glacial Maximum as seen from alkenone paleothermometry. Paleoceanography 24, PA4207.

Enberg, S., Majaneva, M., Autio, R., Blomster, J., Rintala, J.-M., 2018. Phases of microalgal succession in sea ice and the water column in the Baltic Sea from autumn to spring. Marine Ecology Progress Series 599, 19–34.

Endo, H., Ogata, H., Suzuki, K., 2018. Contrasting biogeography and diversity patterns between diatoms and haptophytes in the central Pacific Ocean. Scientific Reports 8, 10916.

Filippova, A., Kienast, M., Frank, M., Schneider, R., 2016. Alkenone paleothermometry in the North Atlantic: A review and synthesis of surface sediment data and calibrations. Geochemistry, Geophysics, Geosystems 17, 1370–1382.

Fisher, N.S., Honjo, S., 1989. Intraspecific differences in temperature and salinity responses in the coccolithophore *Emiliania huxleyi*. Biological Oceanography 6, 355–361.

Guillard, R.R.L., 1975. Culture of phytoplankton for feeding marine invertebrates. In: Smith, W.L., Chanley, M.H. (Eds.), Culture of Marine Invertebrate Animals. Plenum Press, New York, USA, pp. 26–60.

Harada, N., Shin, K.H., Murata, A., Uchida, M., Nakatani, T., 2003. Characteristics of alkenones synthesized by a bloom of *Emiliania huxleyi* in the Bering Sea. Geochimica et Cosmochimica Acta 67, 1507–1519.

Harada, N., Sato, M., Sakamoto, T., 2008. Freshwater impacts recorded in tetraunsaturated alkenones and alkenone sea surface temperatures from the Okhotsk Sea across millennial-scale cycles. Paleoceanography 23, 14.

Harada, N., Sato, M., Oguri, K., Hagino, K., Okazaki, Y., Katsuki, K., Tsuji, Y., Shin, K.H., Tadai, O., Saitoh, S.I., 2012. Enhancement of coccolithophorid blooms in the Bering Sea by recent environmental changes. Global Biogeochemical Cycles 26. https://doi.org/10.1029/2011GB004177.

Ishiwatari, R., Houtatsu, M., Okada, H., 2001. Alkenone-sea surface temperatures in the Japan Sea over the past 36 kyr: warm temperatures at the last glacial maximum. Organic Geochemistry 32, 57–67.

Jaraula, C.M.B., Brassell, S.C., Morgan-Kiss, R.M., Doran, P.T., Kenig, F., 2010. Origin and tentative identification of tri to pentaunsaturated ketones in sediments from Lake Fryxell, East Antarctica. Organic Geochemistry 41, 386–397.

Kaiser, J., Wang, K.J., Rott, D., Li, G., Zheng, Y., Amaral-Zettler, L., Arz, H.W., Huang, Y., 2019. Changes in long chain alkenone distributions and Isochrysidales groups along the Baltic Sea salinity gradient. Organic Geochemistry 127, 92–103.

Langer, G., Benner, I., 2009. Effect of elevated nitrate concentration on calcification in *Emiliania huxleyi*. Journal of Nannoplankton Research 30, 77–80.

Liao, S., Huang, Y., 2022. Group 2i Isochrysidales flourishes at exceedingly low growth temperatures (0 to 6 °C). Organic Geochemistry 174, 104512.

Liao, S., Yao, Y., Wang, L., Wang, K.J., Amaral-Zettler, L., Longo, W.M., Huang, Y., 2020. C_{41} methyl and C_{42} ethyl alkenones are biomarkers for Group II Isochrysidales. Organic Geochemistry 147, 104081.

Liao, S., Wang, K.J., Huang, Y., 2021. Extended chain length alkenoates differentiate three Isochrysidales groups. Organic Geochemistry 161, 104303.

Longo, W.M., Theroux, S., Giblin, A.E., Zheng, Y.S., Dillon, J.T., Huang, Y.S., 2016. Temperature calibration and phylogenetically distinct distributions for freshwater alkenones: Evidence from northern Alaskan lakes. Geochimica et Cosmochimica Acta 180, 177–196.

Longo, W.M., Huang, Y., Russell, J.M., Morrill, C., Daniels, W.C., Giblin, A.E., Crowther, J., 2020. Insolation and greenhouse gases drove Holocene winter and spring warming in Arctic Alaska. Quaternary Science Reviews 242, 106438.

Max, L., Lembke-Jene, L., Zou, J., Shi, X., Tiedemann, R., 2020. Evaluation of reconstructed sea surface temperatures based on $U^{K'}_{37}$ from sediment surface samples of the North Pacific. Quaternary Science Reviews 243, 106496.

Méheust, M., Fahl, K., Stein, R., 2013. Variability in modern sea surface temperature, sea ice and terrigenous input in the sub-polar North Pacific and Bering Sea: Reconstruction from biomarker data. Organic Geochemistry 57, 54–64.

Müller, P.J., Kirst, G., Ruhland, G., von Storch, I., Rosell-Melé, A., 1998. Calibration of the alkenone paleotemperature index $U^{K'}_{37}$ based on core-tops from the eastern South Atlantic and the global ocean (60°N-60°S). Geochimica et Cosmochimica Acta 62, 1757–1772.

Novak, J., McGrath, S.M., Wang, K.J., Liao, S., Clemens, S.C., Kuhnt, W., Huang, Y., 2022. $U^{K'}_{38Me}$ expands the linear dynamic range of the alkenone sea surface temperature proxy. Geochimica et Cosmochimica Acta 328, 207–220.

Peng, G., Meier, W.N., Scott, D.J., Savoie, M.H., 2013. A long-term and reproducible passive microwave sea ice concentration data record for climate studies and monitoring. Earth System Science Data 5, 311–318.

Plancq, J., Couto, J.M., Ijaz, U.Z., Leavitt, P.R., Toney, J.L., 2019. Next-generation sequencing to identify lacustrine haptophytes in the Canadian Prairies: Significance for temperature proxy applications. Journal of Geophysical Research. Biogeosciences 124, 2144–2158.

Prahl, F.G., Wakeham, S.G., 1987. Calibration of unsaturation patterns in long-chain ketone compositions for paleotemperature assessment. Nature 330, 367–369.

Prahl, F.G., Muehlhausen, L.A., Zahnle, D.L., 1988. Further evaluation of long-chain alkenones as indicators of paleoceanographic conditions. Geochimica et Cosmochimica Acta 52, 2303–2310.

Prahl, F.G., Rontani, J.F., Zabeti, N., Walinsky, S.E., Sparrow, M.A., 2010. Systematic pattern in $U^{K'}_{37}$ – Temperature residuals for surface sediments from high latitude and other oceanographic settings. Geochimica et Cosmochimica Acta 74, 131–143.

Randlett, M.E., Coolen, M.J.L., Stockhecke, M., Pickarski, N., Litt, T., Balkema, C., Kwiecien, O., Tomonaga, Y., Wehrli, B., Schubert, C.J., 2014. Alkenone distribution in Lake Van sediment over the last 270 ka: influence of temperature and haptophyte species composition. Quaternary Science Reviews 104, 53–62.

Rosell-Melé, A., 1998. Interhemispheric appraisal of the value of alkenone indices as temperature and salinity proxies in high-latitude locations. Paleoceanography 13, 694–703.

Rosell-Melé, A., Comes, P., 1999. Evidence for a warm Last Glacial Maximum in the Nordic seas or an example of shortcomings in $U^{K'}_{37}$ and U^{K}_{37} to estimate low sea surface temperature? Paleoceanography 14, 770–776.

Rosell-Melé, A., Balestra, B., Kornilova, O., McClymont, E., Russell, M., Monechi, S., Troelstra, S., Ziveri, P., 2011. Alkenones and coccoliths in ice-rafted debris during the Last Glacial Maximum in the North Atlantic: implications for the use of $U^{K'}_{37}$ as a sea surface temperature proxy. Journal of Quaternary Science 26, 657–664.

Saruwatari, K., Satoh, M., Harada, N., Suzuki, I., Shiraiwa, Y., 2016. Change in coccolith size and morphology due to response to temperature and salinity in coccolithophore *Emiliania huxleyi* (Haptophyta) isolated from the Bering and Chukchi seas. Biogeosciences 13, 2743–2755.

Schouten, S., Ossebaar, J., Schreiber, K., Kienhuis, M., Langer, G., Benthien, A., Bijma, J., 2006. The effect of temperature, salinity and growth rate on the stable hydrogen isotopic composition of long chain alkenones produced by *Emiliania huxleyi* and *Gephyrocapsa oceanica*. Biogeosciences 3, 113–119.

Sicre, M.A., Bard, E., Ezat, U., Rostek, F., 2002. Alkenone distributions in the North Atlantic and Nordic sea surface waters. Geochemistry, Geophysics, Geosystems 3. https://doi.org/10.1029/2001GC000159.

Sikes, E.L., Sicre, M.A., 2002. Relationship of the tetra-unsaturated C_{37} alkenone to salinity and temperature: Implications for paleoproxy applications. Geochemistry, Geophysics, Geosystems 3, 1–11.

Stephens, C., Levitus, S., 2002. World Ocean Atlas 2001. Volume 1, Temperature.

Theroux, S., D'Andrea, W.J., Toney, J., Amaral-Zettler, L., Huang, Y., 2010. Phylogenetic diversity and evolutionary relatedness of alkenone-producing haptophyte algae in lakes: Implications for continental paleotemperature reconstructions. Earth and Planetary Science Letters 300, 311–320.

Theroux, S., Huang, Y., Toney, J.L., Andersen, R., Nyren, P., Bohn, R., Salacup, J., Murphy, L., Amaral-Zettler, L., 2020. Successional blooms of alkenone-producing haptophytes in Lake George, North Dakota: Implications for continental paleoclimate reconstructions. Limnology and Oceanography 65, 413–425.

Tierney, J.E., Tingley, M.P., 2018. BAYSPLINE: A new calibration for the alkenone paleothermometer. Paleoceanography and Paleoclimatology 33, 281–301.

Versteegh, G.J., Riegman, R., de Leeuw, J.W., Jansen, J.H.F.F., 2001. $U^{K'}_{37}$ values for *Isochrysis galbana* as a function of culture temperature, light intensity and nutrient concentrations. Organic Geochemistry 32, 785–794.

Wang, K.J., Huang, Y., Majaneva, M., Belt, S.T., Liao, S., Novak, J., Kartzinel, T.R., Herbert, T.D., Richter, N., Cabedo-Sanz, P., 2021. Group 2i Isochrysidales produce characteristic alkenones reflecting sea ice distribution. Nature Communications 12, 1–10.

Yao, Y., Zhao, J., Longo, W.M., Li, G., Wang, X., Vachula, R.S., Wang, K.J., Huang, Y., 2019. New insights into environmental controls on the occurrence and abundance of Group I alkenones and their paleoclimate applications: Evidence from volcanic lakes of northeastern China. Earth and Planetary Science Letters 527, 115792.

Yao, Y., Zhao, J., Vachula, R.S., Liao, S., Li, G., Pearson, E.J., Huang, Y., 2022. Phylogeny, alkenone profiles and ecology of Isochrysidales subclades in saline lakes: Implications for paleosalinity and paleotemperature reconstructions. Geochimica et et Cosmochimica Acta 317, 472–487.

Zheng, Y.S., Heng, P., Conte, M.H., Vachula, R.S., Huang, Y.S., 2019. Systematic chemotaxonomic profiling and novel paleotemperature indices based on alkenones and alkenoates: Potential for disentangling mixed species input. Organic Geochemistry 128, 26–41.

Zheng, Y., Huang, Y., Andersen, R.A., Amaral-Zettler, L.A., 2016. Excluding the di-unsaturated alkenone in the U^{K}_{37} index strengthens temperature correlation for the common lacustrine and brackish-water haptophytes. Geochimica et Cosmochimica Acta 175, 36–46.

Zheng, Y., Tarozo, R., Huang, Y., 2017. Optimizing chromatographic resolution for simultaneous quantification of long chain alkenones, alkenoates and their double bond positional isomers. Organic Geochemistry 111, 136–143.